A REVISED PHYTOPLANKTON GROWTH EQUATION FOR WATER QUALITY MODELLING IN LAKES AND PONDS

James Kempf, John Casti and Lucien Duckstein
Department of Systems and Industrial Engineering
University of Arizona
Tucson, Arizona 85721

Abstract

A physiological model of nutrient uptake, based on membrane transport is combined with a phytoplankton biomass growth equation, based on internal nutrient limitation, to form a system of equations modeling phytoplankton growth which are capable of considerably richer dynamics than the Michaelis-Menton-Monod model (M^3) or the Droop model. In particular, since the characteristic time scale of nutrient uptake is considerably faster than that of biomass increase, a singular perturbation problem results, leading to a relaxation oscillation similar to the van der Pol oscillator. In contrast with both the Michaelis-Menton-Monod model and the Droop model, which were developed using steady state chemostat data, the present model would seem to be appropriate for batch cultures and lakes with long turnover times, where the assumptions of the chemostat steady state are not fulfilled. The qualitative behavior of the model compares favorably with data on batch growth of phytoplankton from the literature.

Introduction

Algal cells raised under the physical-chemical conditions which, in the phytoplankton nutrition and aquatic ecosystem modeling literature, are called the chemostat "steady state", are usually quite far from steady state in a physiological sense. The chemostat steady state is maintained by supplying enough nutrient externally so that the internal nutrient concentration of the phytoplankton does not change and harvesting off the resulting growth of phytoplankton, so that the population size remains constant.

If phytoplankton are removed from a chemostat at steady state and allowed to increase in numbers until their internal nutrient supply is exhausted, a quite different type of phytoplankton population results. The final population size is often far higher than that of the chemostat steady state, and the cellular composition of the population is quite different (Bienfang, 1975). A population at physiological equilibrium is more similar to a batch culture in stationary phase, in which the cells may undergo morphological changes when the external and internal nutrient supply is exhausted (Fogg, 1975). This distinction between the chemostat steady state and the physiological steady state is often not clearly drawn in the algal nutrition and aquatic ecosystem modeling literature.

The distinction becomes crucial when modeling lakes with very high turnover times (Hutchinson, 1957) or for explaining algal species succession. In very large lakes and marine environments with low turnover times, the input of nutrients and removal of water containing phytoplankton occurs swiftly enough so that the chemostat is probably a good approximation. In smaller lakes, however, outflows and inflows tend to be restricted, so that turnover times are higher, and the environmental conditions thus seem better approximated by a batch culture.

Similarly, the transition in an algal species succession from one species to another usually occurs when the first species has exhausted the external nutrient supply. Thus the physiological condition of the species being replaced is probably better approximated by that of a stationary phase batch culture than that of a culture at the chemostat steady state, in which the cells are maintained in log phase through nutrient input.

The two most widely used models for nutrient limited phytoplankton growth, the Michaelis-Menton-Monod model (M^3) (DiToro et al., 1971, 1977) and the Droop internal nutrient model (Rhee, 1980) were both developed using experimental data from chemostat experiments. In both models, the specific growth rate of the phytoplankton population, μ, is a rectangular hyperbolic function of a nutrient concentration, q; being approximately linear in q for q small and approximately constant in q for q large. The difference is that, for the M^3 model, q is the external nutrient concentration, while for the Droop model, q is the internal concentration or cell quota. In addition, the specific growth rate becomes negative in the internal nutrient model, if q falls below q_0, which is taken to be the level of q necessary for maintaining the cell's metabolic machinery in good order.

The internal nutrient model also requires an equation for the rate of nutrient uptake by the cell, and, in most cases, this is also of a rectangular hyperbolic form in the external nutrient concentration. When both models are examined analytically near the chemostat steady state, the resulting dynamical behavior is quite similar (DiToro, 1980), suggesting that the M^3 model would be the better choice, since it is the simpler.

In this paper, a model of phytoplankton nutrient uptake and growth, based on a simplified model of nutrient uptake, is developed and examined numerically and analytically. The potential for relaxation oscillations similar to those in the van der Pol equation (Howard, 1979) or those discovered in a model for a grazing ecosystem (May, 1977; Kempf, 1981) is demonstrated numerically and a lower bound on the total nutrient in the culture or ecosystem is derived, above which relaxation oscillations can occur. Numerical integration of the model results in a trajectory which is qualitatively similar to the results of a batch experiment (DeMarche et al., 1979) that measured internal nitrate concentration, and also to a case from the literature in which no measurement of internal nutrient concentration was made (Fogg, 1975) but which displayed an oscillating population size during the stationary phase of a batch culture. The implications for aquatic ecosystem modeling, in particular, and theoretical ecology, in general, are discussed.

The Model

The transport of nutrient across the algal cell membrane is a crucial step in nutrient uptake. Membrane transport can be separated into two types, depending on whether or not the cell expends energy to facilitate the flow of transported substances. If the process occurs strictly as a result of the electrochemical gradient for the transported substance, then transport is passive, while if energy is expended in the transport of the substance itself or to maintain an ionic gradient for a co-transported solute, the term active transport is used. Membrane transport is perhaps best understood for the sodium-potassium ion pump in nerve cells (Hodgkin, 1964); but for phytoplankton nutrient transport, there is very little specific data.

Various models have been developed to explain both passive and active transport. The most widely accepted is that enzymatic type proteins within the cell membrane latch onto substances outside the cell and either migrate across the cell membrane or change shape so that the portion of the molecule carrying the bound substance protrudes into the cytoplasm, where the substance is released. In active transport, the affinity of the membrane protein for the transported substance is assumed to be enhanced either through the hydrolysis of ATP or through the binding of a co-transported solute (Heinz, 1978). Mathematical models for both passive transport (Heinz, 1978) and active transport (Verhoff and Sudaresan, 1972; Heinz, 1978) have been developed.

In contrast with the above models, an experimental system with glucose pumping activity has been demonstrated in which no movement of a membrane protein is involved. The system consists of a membrane in which two enzymes (a hexokinase and a phosphatase) are immobilized between two layers of a material impermeable to the enzymes' common intermediate (Thomas, 1976). When the membrane is charged with ATP, glucose is pumped from the hexokinase side to the phosphatase side without any translocation of membrane proteins. A mathematical model of this system, based on reaction-diffusion equations, has also been developed and studied both numerically and analytically (Kernevez, 1980).

Rather than embrace any of the above formulations, general dynamical features of phytoplankton nutrient uptake and mass balance considerations will be used to develop the nutrient uptake equation. Evidence exists that phosphate is transported actively in Nitella translucens (Kuhl, 1974) and other species and that assimilation of nitrate and ammonia also requires ATP (Morris, 1974); however, since the exact nature of the mechanism behind active transport is not too well known in general (and may, in fact, be quite different for different types of transported solutes), it seems safer to base the model on the general dynamics of the process rather than on any particular mechanism.

Considering, for the moment, that no conversion of internal nutrient into cell material is taking place, the net flow of nutrient across the cell membrane will be the difference between the gross flux and the backward leakage rate (Heinz, 1978):

$$\dot{q} = \text{gross uptake rate} - \text{backward leakage rate}$$

where

$$q = \text{internal cellular nutrient concentration } (\text{wt}\cdot\text{vl}^{-1}\cdot\text{cell}^{-1})$$

Data from short term uptake experiments indicates that the gross uptake rate is approximately Michaelis-Menton in form in the external nutrient concentration, n (Rhee, 1980). Theoretical considerations also suggest that the gross uptake rate probably obeys Michaelis-Menton kinetics, since enzymatic

type proteins are probably involved in the forward transport process (Heinz, 1978).

Since phytoplankton have been observed, both in culture and in nature, to concentrate nutrient very strongly against the electrochemical gradient (Rhee, 1973; Bienfang, 1975), a Michaelis-Menton form for the backward leakage reaction seems inappropriate. A more likely possibility is that the backward leakage reaction is substrate inhibited, so that at very high internal nutrient concentrations, the leakage rate decreases rather than saturating to some maximum rate. The leakage rate would thus be approximately linear in q, for q near zero, achieve a maximum, for some intermediate q, and decrease toward zero, as q approaches infinity (see Fig. 1). Such substrate inhibited kinetics are displayed by the uricase reaction, in which uric acid is converted by the enzyme uricase into allantoin in the presence of oxygen (Kernevez, 1980). If substrate inhibited kinetics are assumed for the leakage rate, then the equation for uptake takes the form:

$$\dot{q} = \frac{v_n \cdot n}{(K_n + n)} - \frac{v_q \cdot q}{[K_q + q(1 + \frac{q}{K_I})]} \tag{1}$$

where v_n, v_q = respective maximum uptake rates ($wt \cdot vl^{-1} \cdot time^{-1}$)

K_I = inhibition constant ($wt \cdot vl^{-1} \cdot cell^{-1}$)

K_n, K_q = respective half saturation constants ($wt \cdot vl^{-1} \cdot cell^{-1}$)

Removing the assumption that no conversion of internal nutrient into cell material is taking place, the growth of particulate or fixed nutrient, p, will take place at a rate of $\mu \cdot p$ $wt \cdot vl^{-1} \cdot time^{-1}$, where μ is the specific growth rate of the phytoplankton population. Thus the cell pool will be "thinned out" at a rate equal to $\mu \cdot q$ $wt \cdot vl^{-1} \cdot cell^{-1} \cdot time^{-1}$. Including this term in Eq. 1 gives the final equation for the change in the cell pool:

$$\dot{q} = \frac{v_n \cdot n}{(K_n + n)} - \frac{v_q \cdot q}{(K_q + q + \frac{q^2}{K_I})} - \mu q \tag{2}$$

Before proceeding further it might be helpful to summarize the two assumptions made in developing Eq. 2:

(1) The uptake rate is the difference between a forward transport rate and a backward leakage rate. This is in contrast to most developments in the literature (Rhee, 1980) which assume that the uptake rate is Michaelis-Menton in external nutrient, with perhaps an inhibition term due to increasing internal nutrient concentration, but in line with more general modeling of passive and active transport processes (Heinz, 1979).

(2) The gross uptake rate is Michaelis-Menton and the backward leakage rate is substrate inhibited. Both assumptions seem reasonable from a physiological standpoint, and are supported by general dynamic considerations (i.e., the ability of phytoplankton to concentrate nutrient strongly), although further experiments would be the only way to confirm this.

The functional form of the specific growth rate, μ, was left unspecified in the above discussion. A reasonable form, developed by Droop (Rhee, 1980), expresses the specific growth rate as a saturating function of q, which becomes negative if q falls below a cellular maintenance concentration. The equation for the increase in particulate or fixed nutrient would then be

$$\dot{p} = \mu_m(1 - \frac{q_0}{q}) \cdot p = \mu p \tag{3}$$

where μ_m = maximum growth rate ($time^{-1}$)

q_0 = maintenance level of cellular pool ($wt \cdot vl^{-1} \cdot cell^{-1}$)

p = particulate or fixed nutrient ($wt \cdot vl^{-1}$)

In batch culture or in lakes with long turnover times, the total amount of nutrient in the system will be constant. Thus, assuming the lake or culture volume is constant, the sum of the external concentration, the total internal pool concentration, and the particulate concentration must be constant, in order to assure mass balance:

$$n + a \cdot q \cdot p + p = n_T \tag{4}$$

where n_T = total system nutrient concentration ($wt \cdot vl^{-1}$)

a = volume density of the cell ($vl \cdot cell \cdot wt^{-1}$); (e.g., reciprical of the fraction of cell volume which is protein)

To facilitate the analysis, it is helpful if all the variables and parameters are rendered dimensionless, so comparisons between quantities are about at the same order of magnitude (Fife, 1979). Let $\underline{q} = \frac{q}{K_q}$, $P = \frac{P}{K_n}$, $\underline{n} = \frac{n}{K_n}$, and $\tau = t \cdot \mu_m$, Eqs. 2 and 3 become:

$$\dot{P} = (1 - \frac{\alpha}{\underline{q}}) \cdot P = \mu P \tag{5a}$$

$$\dot{\underline{q}} = \frac{\beta \cdot \underline{n}}{(1 + \underline{n})} - \frac{\gamma \cdot \underline{q}}{(1 + \underline{q} + k\underline{q}^2)} - \mu \underline{q} \tag{5b}$$

where $\alpha = \frac{q_0}{K_q}$, $\beta = v_n(\frac{1}{K_q \mu_m})$, $\gamma = v_q(\frac{1}{K_q \mu_m})$, and $k = \frac{K_q}{K_I}$. $\dot{A}$ now means derivative with respect to τ.

To convert Eq. 4 to dimensionless form, note that if the volume density of the cell, a, is assumed constant, then Eq. 4 becomes:

$$N_T = \underline{n} + \omega Q + P \tag{5c}$$

where $\omega = aK_q$ and $N_T = \frac{n_T}{K_n}$; and $Q = P \cdot \underline{q}$ is the nondimensional total cellular pool.

The nondimensional external nutrient concentration, $\underline{n}$, can be eliminated from Eq. 5b by solving Eq. 5c for $\underline{n}$ and substituting:

$$\dot{\underline{q}} = \frac{\beta(N_T - \omega Q - P)}{(1 + N_T - \omega Q - P)} - \frac{\gamma \underline{q}}{(1 + \underline{q} + k\underline{q}^2)} - \mu \underline{q} \tag{6}$$

Eqs. 5a and 6 can be rendered entirely in terms of Q by substituting $\underline{q} = \frac{Q}{P}$ and using the chain rule to calculate $\dot{Q}$. The resulting equation system will be

$$\dot{P} = (1 - \frac{\alpha P}{Q}) \cdot P \tag{7a}$$

$$\dot{Q} = \left(\frac{\beta(N_T - \omega Q - P)}{(1 + N_T - \omega Q - P)} - \frac{\gamma PQ}{(P^2 + PQ + kQ^2)} \right) \cdot P \tag{7b}$$

Bifurcation Geometry

Experimental evidence (Droop, 1973; DiToro, 1980; Rhee, 1980) indicates that nutrient uptake is often an order of magnitude or more faster than growth. Since the characteristic time of Eqs. 7 will be that of the growth reaction, β and γ will be very large. Dividing both sides of Eq. 7b by β, the system becomes (Fife, 1979):

$$\dot{P} = (1 - \alpha \frac{P}{Q}) \cdot P \tag{8a}$$

$$\varepsilon \dot{Q} = \left(\frac{N_T - \omega Q - P}{(1 + N_T - \omega Q - P)} - \frac{\sigma PQ}{(P^2 + PQ + kQ^2)} \right) \cdot P \tag{8b}$$

where $\sigma = \frac{\gamma}{\beta}$ and $\varepsilon = \frac{1}{\beta} << 1$.

Eqs. 8a and 8b constitute a singular perturbation problem, since the time derivative of Q is multiplied by a small parameter. In the next section the dynamics of the system are described, using a nonstandard approach advocated in Diener and Poston (1980) and Lutz and Goze (1982), and the existence

of a relaxation type oscillation is demonstrated. In order for a relaxation type oscillation to be possible, however, the zero set of Eq. 8b must have the folded structure shown in Fig. 2.

The zero set of Eq. 8b will be given by:

$$\Gamma = \{(P,Q): \frac{N_T - \omega Q - P}{(1 + N_T - \omega Q - P)} - \frac{\sigma PQ}{(P^2 + PQ + kQ^2)} = 0\} \tag{9}$$

$$\Gamma = \{(P,Q): h(P,Q) - g(P,Q) = f(P,Q) = 0\}$$

Since the characteristic time scale of Q will be considerably faster than that of P, P can be considered a parameter for purposes of examining the geometry of Γ. Because of the difference in time scales, Γ is often called the slow manifold (Zeeman, 1977).

Kubicek's method of continuation (Kubicek, 1976; Kernevez, 1980) was used to numerically calculate Γ for appropriate parameter values (see Fig. 2). The method of continuation forms a set of differential equations for P and Q using the arc length along the curve as the independent variable. The equations are numerically integrated from a known point using the Adams-Bashforth method with maximal order four and a variable step size. A correction step using Newton's method follows the integration. Details can be found in Kernevez (1980).

The points (P^*,Q^*) and (P^{**}, Q^{**}) in Fig. 2 will be such that:

$$(P^*,Q^*),(P^{**},Q^{**}) \in \Gamma \tag{10}$$

$$(P^*,Q^*),(P^{**},Q^{**}) \in \{(P,Q): \frac{\partial f}{\partial Q} = 0\}$$

Following Stewart (1976) and Poston and Stewart (1978), these points will be called fold points. An analytical solution of the two conditions in Eq. 10 for the fold points is impossible; however, the bifurcation geometry of Γ can be studied using an approach similar to that in Kernevez (1980).

For a particular species of algae, the parameters α, β, γ, ω, and k will only change slightly with temperature. The parameter which is most likely to determine whether or not Γ has the folded structure necessary for relaxation oscillations is therefore N_T. Changes in N_T will correspond to changes in the trophic state of the lake or other experimental system under investigation, and therefore the bifurcation geometry of Γ with changes in N_T will give information on how the dynamics of a particular algal species can change with trophic state.

From Eq. 9, if $(P,Q) \in \Gamma$ then

$$(P,Q) \in \{(P,Q): h(P,Q) = g(P,Q)\}$$

This means that points on Γ will occur when the uptake function, h, and the leakage function, g, are equal. Considering g, Fig. 1 shows that, for a fixed value of P, g will achieve a maximum at some Q_m^g and will approach zero as Q approaches infinity. On the other hand, h will be monotonically decreasing in both P and Q, as can be seen by examining its derivatives:

$$\frac{\partial h}{\partial P} = \frac{-1}{(1 + N_T - \omega Q - P)^2} \tag{11a}$$

$$\frac{\partial h}{\partial Q} = \frac{-\omega}{(1 + N_T - \omega Q - P)^2} \tag{11b}$$

Thus, if P is considered to be a slowly varying parameter, h will have a maximum when P = 0 and Q = 0 and will decrease thereafter.

To motivate the following theorem, consider Figs. 3a and 3b, which show how Γ could <u>not</u> have two fold points. Let the points on the graph of g and h where g and h achieve their maximum be called g_m

and h_m, respectively. Then, as shown in Fig. 3a, if g_m is above h_m for all values of P and Q, the only intersection point between the two will be on the tail of g. Similarly, if P_i^{hg} is the value of P where the graph of g, at its inflection point, intersects the graph of h and if P_m^{hg} is the value of P where the graph of g, at its maximum, intersects the graph of h, then if $P_i^{hg} < P_m^{hg}$, only one intersection will occur, as shown in Fig. 3b.

From the above comments, the following two criteria must be satisfied in order for three intersections between h and g to occur:

(1) $g_m < h_m$

(2) $P_m^{hg} < P_i^{hg}$

The sequence in Fig. 4 shows how, for increasing P, three such intersections are generated.

These conditions on g_m, h_m, P_m^{hg}, and P_i^{hg} are translated into conditions on the bifurcation parameter N_T by the following theorem:

Theorem 1: In order for Γ to exhibit two fold points, N_T must satisfy:

$$N_T > \max[N_1, N_2] \tag{12}$$

where

$$N_1 = \frac{\sigma}{2\kappa + (1 - \sigma)}$$

$$N_2 = \frac{\sigma}{(1 - 2\eta)\,\omega} \frac{(\kappa + 2\eta\omega)}{[2\kappa + (1 - \sigma)]} - \frac{2\eta(\kappa + \omega)}{[\kappa + 2\eta(1 - \sigma) + 4\kappa\eta^2]}$$

$$\eta = \cos\{\tfrac{1}{3}\cos^{-1}(\tfrac{1}{2\kappa})\} \qquad k > \tfrac{1}{4} \qquad \kappa = \sqrt{k}$$

Remark: For the values of the parameters used to generate Fig. 4, namely $\sigma = 4.9$, $k=9$, $\omega = 0.5$, $N_T = 5$:

$$N_1 = 2.33 \qquad N_2 = -4.594 \tag{13}$$

and since $N_T = 5$, Inequality (12) is satisfied.

Proof: With respect to the conditions in Points (1) and (2) above, the equations for g and h can be solved for g_m, h_m, P_m^{hg}, and P_i^{hg} in the following way.

Considering P as being fixed and differentiating g once with respect to Q gives:

$$\frac{\partial g}{\partial Q} = \frac{\sigma P(P^2 - kQ^2)}{(P^2 + PQ + kQ^2)^2} \tag{14}$$

Setting Eq. 14 to zero and solving for Q as a function of P gives:

$$Q_m^g = \frac{P_m^g}{\kappa} \tag{15}$$

At which g will have the value:

$$g_m = \frac{\sigma}{2\kappa + 1} \tag{16}$$

Note that Q_m^g will be monotonically increasing with P, so that Q_m^g will move to the right as P increases. On the other hand, g_m will be fixed with respect to changes in P.

Differentiating g again with respect to Q gives:

$$\frac{\partial^2 g}{\partial Q^2} = \sigma P \left(\frac{(2k^2 Q^3 - 6kQP^2 - 2P^3)}{(P^2 + PQ + kQ^2)^3} \right) \tag{17}$$

Inflection points will occur where $\frac{\partial^2 g}{\partial Q^2}$ is zero. Setting Eq. 17 to zero gives the following zero set:

$$Q_i^{g\,3} - \frac{3}{k} Q_i^g P_i^{g\,2} - \frac{P_i^{g\,3}}{k^2} = 0 \tag{18}$$

This cubic will have three real roots if the cubic discriminant is less than zero:

$$\frac{1}{4k^4} - \frac{1}{k^3} < 0 \tag{19}$$

Solving for k gives:

$$k > \frac{1}{4} \tag{20}$$

which is the condition on k in the statement of the thorem.

The middle root of the cubic in (18) will be given by:

$$Q_i^g = \frac{2P_i^g}{\kappa} \cos \left\{ \frac{1}{3} \cos^{-1} \left(\frac{1}{2\kappa} \right) \right\} \tag{21}$$

$$Q_i^g = \frac{2P_i^g}{\kappa} \cdot \eta$$

Again, Q_i^g will be monotone increasing with P.

The value of g at the inflection point will be

$$g_i = \frac{2\sigma\eta}{(\kappa + 2\eta + 4\kappa\eta^2)} \tag{22}$$

which is, again, constant with respect to changes in P.

At P = 0, Q = 0, h achieves its maximum:

$$h_m = \frac{N_T}{1 + N_T} \tag{23}$$

Substituting (16) and (23) into the condition in Point (1) gives:

$$\frac{\sigma}{2\kappa + 1} < \frac{N_T}{1 + N_T} \tag{24}$$

Solving for N_T gives N_1 in (12).

P_m^{hg} can be found by equating g_m and h_m at $Q = Q_m^g$:

$$\frac{\sigma}{2\kappa + 1} = \frac{N_T - P_m^{hg}(1 + \frac{\omega}{\kappa})}{[1 + N_T - P_m^{hg}(1 + \frac{\omega}{\kappa})]} \tag{25}$$

or

$$P_m^{hg} = \frac{\kappa}{\kappa + \omega}\left(N_T - \frac{\sigma}{[2\kappa + (1 - \sigma)]}\right) \tag{26}$$

P_i^{hg} can be found in a similar way:

$$\frac{2\sigma\eta}{(\kappa + 2\eta + 4\kappa\eta^2)} = \frac{N_T - P_i^{hg}(1 + 2\frac{\eta}{\kappa})}{[1 + N_T - P_i^{hg}(1 + 2\frac{\eta}{\kappa})]} \tag{27}$$

or

$$P_i^{hg} = \frac{\kappa}{\kappa + 2\eta\omega}\left(N_T - \frac{2\sigma\eta}{[\kappa + 2\eta(1 - \sigma) + 4\kappa\eta^2]}\right) \tag{28}$$

The inequality in Point (2) would then be:

$$\frac{\kappa}{\kappa+\omega}\left(N_T - \frac{\sigma}{[2\kappa+(1-\sigma)]}\right) < \frac{\kappa}{\kappa+2\eta\omega}\left(N_T - \frac{2\sigma\eta}{[\kappa+2\ (1-\sigma)+4\kappa\eta^2]}\right) \tag{29}$$

Solving for N_T gives N_2 in (12).

An additional condition for relaxation oscillations is that the $\dot{P} = 0$ isocline intersect the slow manifold on the unstable section between the fold points, as shown in Fig. 5. If the intersection point between Γ and the set:

$$\Lambda = \{(P,Q):\ P = \frac{1}{\alpha}Q\} = \{(P,Q):\ \dot{P} = 0,\ P \neq 0\} \tag{30}$$

is denoted by (P_I,Q_I), then the condition for relaxation oscillation is:

$$Q^* < Q_I < Q^{**} \qquad P^* < P_I < P^{**} \tag{31}$$

The following theorem gives Q_I as a function of the parameters:

$$Q_I = \frac{\alpha[N_T\{k\omega(\alpha k - 1) + (1 - \sigma)\} - \sigma]}{[\kappa\omega(\alpha^2 + \alpha - 1) + \alpha(\omega - \sigma) - (\sigma - 1)]} \tag{32}$$

Proof: Since $Q_I \varepsilon \{\Lambda \cap \Gamma\}$, substituting the value of P in (30) into the equation for Γ gives:

$$\kappa\omega Q_I^3 + \{\frac{Q_I}{\alpha}[\omega+\sigma(1-\frac{1}{\alpha})+k+\frac{1}{\alpha}] - N_T[k+\frac{\sigma-1}{\alpha}]+\frac{\sigma}{\alpha}\}Q_I^2 + \{N_T - \frac{Q_I}{\alpha}\frac{Q_I^2}{\alpha^2} \tag{33}$$

Factoring out a Q_I^2 and solving for Q_I gives Eq. 33.

Dynamics

As mentioned in the previous section, the singular perturbation problem posed by Eqs. 7 will evolve on two time scales: a fast scale for Q and a slow scale for P. The initial change in Q will be rapid; so that, before P changes appreciably, the trajectory will have already approached to within an infinitesimal distance of Γ.

There are a number of analytical approaches which have been used to study singular perturbation problems of this type (Fife, 1979; Diener and Poston, 1981; Lutz and Goze, 1982; Nayfeh, 1981). One of the most attractive is nonstandard analysis (Diener and Poston, 1981; Lutz and Goze, 1982). The small parameter ε in Eq. 7b is formally set to an infinitesimal number (Robinson, 1974) instead of considering limiting behavior for small finite ε. While, in the numerical example in Fig. 6, ε is anything but infinitesimal, the use of infinitesimals makes it easier to talk about what happens when a finite ε becomes small. Lutz and Goze (1982) formally prove the existence of relaxation oscillations in systems such as (7), so comments here will be limited to a discussion of the general behavior of the flow in the

state space.

Define the halo of a set, $S \varepsilon \mathbb{R}^n$ as the set of points infinitely near S. Also, with reference to the system in Eqs. 7, define:

$$\Lambda^+ = \{(P,Q): f(P,Q) > 0\} \tag{34a}$$

$$\Lambda^- = \{(P,Q): f(P,Q) < 0\} \tag{34b}$$

and:

$$\Gamma^+ = \{(P,Q): P > \frac{1}{\alpha}Q\} \tag{35a}$$

$$\Gamma^- = \{(P,Q): P < \frac{1}{\alpha}Q\} \tag{35b}$$

Then for $(P,Q)\varepsilon\Lambda^+$, $\dot{Q} > 0$; while for $(P,Q)\varepsilon\Lambda^-$,$\dot{Q} < 0$. Since the $\dot{Q}$ equation will equilibrate much faster than the $\dot{P}$ equation, the flow in the Q direction will be almost perpendicular to the slow manifold, until it is within the halo of the slow manifold. There it will level out and flow along the slow manifold, in the direction of increasing P, if the flow is in Γ^+ or in the direction of decreasing P, if the flow is in Γ^-.

When the flow on the slow manifold reaches the upper fold point at (P^{**},Q^{**}), the fast foliation in the Q direction will push the flow down onto the lower sheet. Here, $\dot{P} < 0$, so the flow will be to the left, in the direction of decreasing P. At the lower fold point, (P*,Q*), the opposite process takes place and the result is a relaxation oscillation, as shown in Fig. 5. Such behavior is called "slaving" by Haken (1978).

Figs. 6 are a numerical integration of Eqs. 7, with $N_T = 5.0$, $\sigma = 4.9$, $\omega = 0.5$, $k = 9.0$, $\alpha = 0.8$, and $\frac{1}{\delta} = 29.5$. Initial conditions were $P(0) = 0.1$ and $Q(0) = 0.1$. Gear's stiffly stable method was used in the integration, since the difference in time scales between the two equations makes the system stiff. The oscillating nature of the solution is obvious both from the flow in the state space, in Fig. 6a, and from the time trajectories, in Figs. 6b and 6c.

Comparison with Experimental Data

DeMarche et al. (1979) report on an experiment in which the diatom Skeletoma costatem was raised in batch culture and both the population size, p, and the internal nutrient pool of nitrate, q, were monitored. Samples of the culture were taken at regular time intervals, and the population size was determined by measuring particulate nitrogen concentration in the samples. The internal nitrate pool concentration was measured by sonicating a portion of the sample and measuring the resulting increase in the medium nitrate concentration.

In Fig. 7, the data of DeMarche et al. (1979) are replotted as a state space plot, with q against p. Initially, the internal nutrient concentration rose very rapidly, over a period of less than 0.2 day, without any change in the population size. The population size then began to increase more slowly; and, as it did so, the internal nitrate concentration also decreased slowly, until about 2.8 day into the experiment. At this point, q decreased quite suddenly to near zero, again over a period of about 0.2 day, while no large change in p occured. The experiment was terminated at this point.

The qualitative similarity between the experimental data, plotted in Fig. 7, and the numerical integration, in Fig. 6, is striking. The fast initial rise in the internal concentration and the drop at the start of the oscillation match in both, as does the movement along the slow manifold. Unfortunately, the experiment was terminated before the oscillation could really develop.

Fig. 8 displays the results of an experiment in which log phase Monodus subtemaneus cells were transferred into a medium containing no nitrogen (Fogg, 1975). After the internal nitrogen pool was exhausted, the population size began to oscillate. Since the cells initially had no external nitrogen source, the oscillation developed sooner than would have been the case if nitrogen had been available.

Discussion

In aquatic ecosystem models which use the M^3 model or the Droop model, it is not possible to obtain an unforced limit cycle or relaxation oscillation without another "external" state variable. Addition of another trophic level, for example, zooplankton predators, can lead to population cycles of a predator-prey type (Adachi and Ikeda, 1978; Arnold, 1978) which have been widely discussed in the theoretical ecological literature (May, 1978). Such a system is ecologically quite distinct from the system presented above, in which a rapid change in the physiological state of a single species is

causing a population cycle.

Another ecosystem in which a physiological variable might be causing oscillations is the cycles of small mammal populations in the Arctic (Finerty, 1980). The lynx-hare pelt data from the Hudson Bay Company records are one of the most widely cited pieces of evidence for limit cycle oscillations in predator-prey systems (but see May (1980) for questions on the data's validity). Statistical examination of the data for a number of small mammal populations in the Arctic (Finerty, 1980) suggests that the predator population cycles are actually being forced by a population cycle in their chief food supply, the Arctic hare, rather than causing the cycle directly. Finerty speculates on a number of possible causes for the hare population cycle, one of which is the kind of physiologically caused periodicity discussed above.

In general, the internal physiological state of an organism would be expected to equilibrate on a more rapid time scale than the reproductive state of the entire population. To the extent that the reproductive state is influenced by the physiological state, a separation of the dynamics might occur, in which the internal physiological state forms a slow manifold upon which the population size evolves.

Wherever the physiological state manifold has a folded structure, like that of the internal nutrient manifold in the above model, the physiological state variable will change rapidly to a new quasi-equilibrium, and the population size will adjust more slowly. Such a phenomenon could also occur between two different species with radically different characteristic growth rates, for example, whales and krill; with the equation for the species having the higher growth rate forming the slow manifold upon which the system evolves.

Thus, coupling between an organism's physiology and the environment might be responsible for extremely complex population dynamics, which have previously been ascribed to general mass action type interactions between organisms at two trophic levels. A three variable system, with one physiological variable forming a slow manifold, might exhibit the type of chaotic dynamics reported by Rössler (1979). Two possible examples might be the bloom-dieoff cycles in eutrophic ponds, reported by Barica (1974), and the annual species succession of phytoplankton in lakes (Hutchinson, 1957). For such systems, the population trajectories would look as if they were being generated by a stochastic process, even though the underlying dynamics were deterministic.

Conclusions

A physiologically derived phytoplankton growth model has been presented in which the phytoplankton population size can exhibit relaxation oscillations for certain values of the parameters. The model approximates conditions in batch culture or in a self-contained lake, for which the total nutrient concentration in the ecosystem is relatively constant. The internal nutrient equation isocline forms a slow manifold, to which the flow of the dynamical system is strongly and quickly attracted, and upon which the system evolves. If the isocline for the phytoplankton population size intersects the slow manifold on the unstable section, oscillations in the population size can occur. Evidence supporting the model was presented from a batch experiment in which both the population size and the internal nutrient concentration were measured, and from the large body of data in the literature on batch growth of phytoplankton, where no internal nutrient concentration measurements were made.

The implications of the model for ecosystem modeling in general have been discussed. A comparison with another system, the Arctic small mammal populations, in which population oscillations occurred was made. The possible role of physiological variables in ecosystem models has also been mentioned.

Acknowledgements

This research was supported by NSF Grant CEE 8110778, "Modern Stability and Dynamical Concepts in Water Resources Management." We also wish to thank Dr. H. Haken of the Institut für Theoretische Physik, Universität Stuttgart, Stuttgart, West Germany, for the opportunity to visit in the summer of 1981, during which many of the seminal ideas in this paper were developed. Dr. Tim Poston also played a large role in clarifying the authors' thoughts on the dynamics of aquatic ecosystems.

References

Adachi, N. and S. Ikeda. 1978. Stability Analysis of Eutrophication Models. IIASA Research Memorandum RM-78-53, International Institute for Applied Systems Analysis, Laxenburg, Austria.

Arnold, E. M. 1978. Aspects of a zooplankton, phytoplankton, phosphorous system. Ecological Modelling, 5:293-300.

Barica, J. 1974. Some observations on the internal recycling, regeneration, and oscillation of dissolved nitrogen and phosphorous in shallow, self-contained lakes. Archives of Hydrobiology 73(3):334-360.

Bienfang, P. 1975. Steady state analysis of nitrate-ammonium assimilation by phytoplankton. Limnology and Oceanography 20:402-411.

DeMarche, J. M., H. C. Curl, Jr., P. W. Lundy and P. L. Donaghay. 1979. The rapid response of the marine diatom Skeletonema costatum to changes in external and internal nutrient concentration. Marine Biology 53:323-333.

Diener, M. and T. Poston. 1982. On the perfect delay convention or the revolt of the slaved variables. To appear in Chaos and Order in Nature, H. Haken, ed., Springer, Heidelberg.

DiToro, D., D. O'Connor and R. Thomann. 1971. A dynamic model of the phytoplankton population in the Sacramento-San Joaquin Delta. Nonequilibrium Systems in Water Chemistry, Advances in Chemistry Series, 106, American Chemical Society, Washington, 131-180.

DiToro, D., R. Thomann, D. O'Connor and J. Mancini. 1977. Esturine phytoplankton biomass models--verication, analysis, and preliminary applications. The Sea 6:969-1020, E. Goldberg, ed., John Wiley, Inc., New York.

DiToro, D. 1980. Applicability of cellular equilibrium and Monod theory to phytoplankton growth kinetics. Ecological Modelling 8:201-218.

Droop, M. R. 1973. Some thoughts on nutrient limitation in algae. Journal of Phycology 9:264-272.

Fife, P. 1979. Mathematical Aspects of Reacting and Diffusing Systems. Lecture Notes in Biomathematics 28, Springer, Heidelberg.

Finerty, J. P. 1980. The Population Ecology of Cycles in Small Mammals. Yale University Press, New Haven, CT.

Fogg, G. E. 1975. Algal Cultures and Phytoplarkton Ecology. University of Wisconsin Press, Madison, WI.

Haken, H. 1978. Synergetics: An Introduction. Springer, Heidelberg.

Heinz, E. 1978. Mechanics and Energetics of Biological Transport. Molecular Biology, Biochemistry, and Biophysics 29, A. Kleinzeller, G. F. Springer, and H. G. Wittman, eds., Springer, Heidelberg.

Hodgkin, A. L. 1964. The Conduction of the Nerve Impulse. Liverpool University Press, Liverpool.

Howard, L. N. 1979. Nonlinear oscillations. Nonlinear Oscillations in Biology, F. C. Hoppenstadt, ed., Lectures in Applied Mathematics 17:1-67, American Mathematical Society, Providence, RI.

Hutchinson, G. E. 1957. A Treatise on Limnology. Wiley, New York.

Kempf, J. 1980. Multiple steady states and catastrophes in ecological models. ISEM Journal 2(3-4): 55-79.

Kernevez, J. P. 1980. Enzyme Mathematics. Studies in Mathematics and its Applications, 10, J. L. Lions, G. Papanicolaov, and R. T. Rockafeller, eds., North Holland, Amsterdam.

Kubicek, M. 1976. Dependence of solution of nonlinear systems on a parameter. ACM Transactions on Mathematical Software 2:98-107.

Kuhl, A. 1974. Phosphorous. Algal Physiology and Biochemistry, Botanical Monographs, 10:636-654, W. Stewart, ed., University of California Press, Berkeley, CA.

Lutz, R. and M. Goze. 1982. Nonstandard Analysis: A Practical Guide with Applications. Lecture Notes in Mathematics, 881, Springer, Heidelberg.

May, R. 1977. Thresholds and breakpoints in ecosystems with a multiplicity of stable states. Nature 269:471-477.

May, R. 1978. Mathematical aspects of the dynamics of animal populations. Studies in Mathematical Biology Part II: Populations and Communities, M.A.A. Studies in Mathematics, 16:317-366, S. A. Levin, ed.

May, R. 1980. Cree-Ojibwa hunting and the hare-lynx cycle. Nature 286:108-109.

Morris, I. 1974. Nitrogen assimilation and protein synthesis. Algal Physiology and Biochemistry, Botanical Monographs 10:583-609, W. Stewart, ed., University of California Press, Berkeley, CA.

Nayfeh, A. H. 1981. Introduction to Perturbation Techniques. Wiley-Interscience, New York.

Poston, T. and I. N. Stewart. 1978. Catastrophe Theory and Its Applications. Pitman, London.

Rhee, G-Y. 1980. Continuous culture in phytoplankton ecology. Advances in Aquatic Microbiology 2:151-204, M. R. Droop and H. W. Jannasch, eds., Academic Press, London.

Robinson, A. 1974. Nonstandard Analysis. Second Edition. Elsevier, New York.

Rőssler, O. 1979. Continuous chaos-four prototype equations. Annals of the New York Academy of Sciences 316:376-392.

Stewart, I. N. 1976. Catastrophe theory and equations of state: the butterfly in the stirred tank. Mathematical Institute, University of Warwick, Coventry, England.

Thomas, D. 1976. Artificial enzyme membranes: transport, memory and oscillating phenomena. Analysis and Control of Immobilized Enzyme Systems, D. Thomas and J. P. Kernevez, eds., North Holland, Amsterdam.

Verhoff, F. H. and K. R. Sundaresan. 1972. A theory of coupled transport in cells. Biochimica et Biophysica Acta, 255:425-441.

Zeeman, C. 1977. Catastrophe Theory: Selected Papers (1972-1977). Addison-Wesley, Reading, MA.

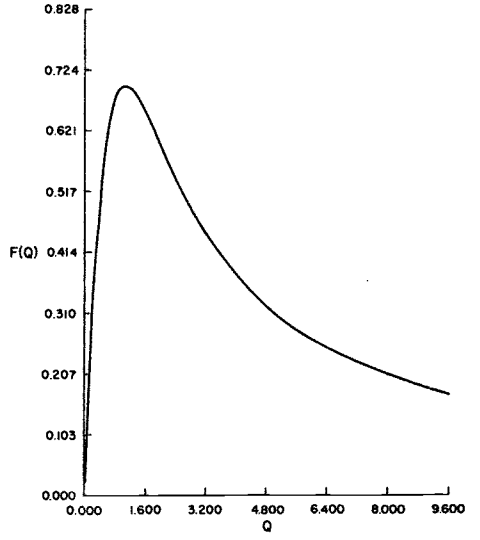

Figure 1. Shape of the substrate inhibited leakage function

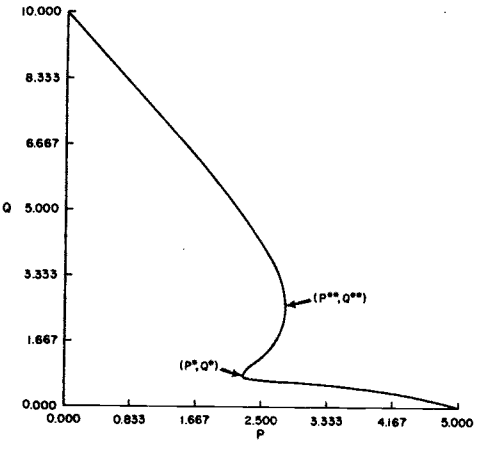

Figure 2. Slow manifold, f(P,Q) = 0, determined by Kubicek's method of continuation for N_T = 5.0, σ = 4.9, ω = 0.5, and k = 9.0

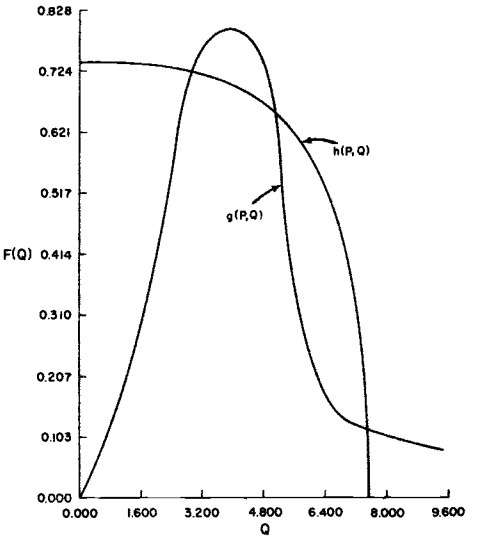

Figure 3a. Relation between g(P,Q) and h(P,Q) for $g_m < h_m$

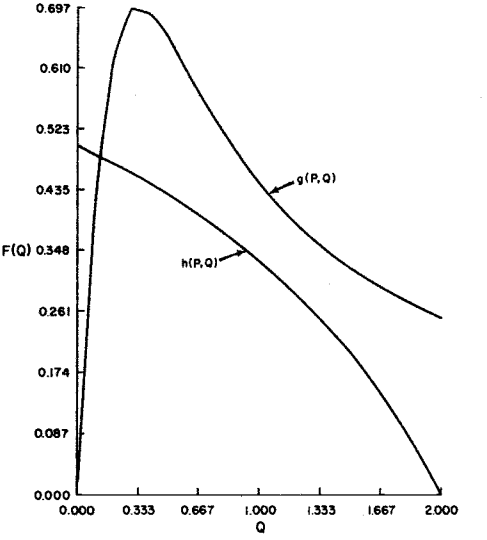

Figure 3b. Relation between g(P,Q) and h(P,Q) for $P_m^{hg} > P_i^{hg}$

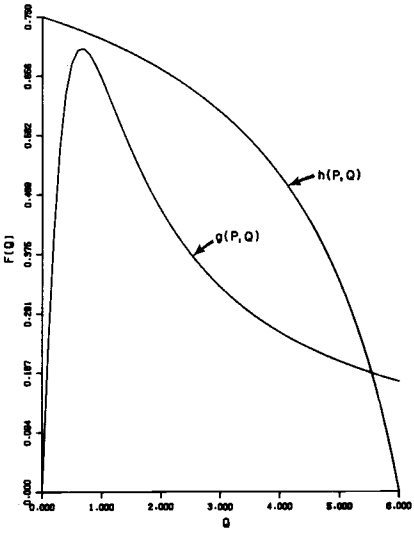

Figure 4a. Relation between g(P,Q) and h(P,Q) for P < P*

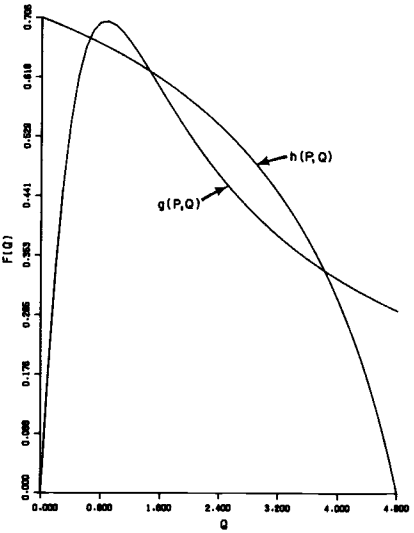

Figure 4b. Relation between g(P,Q) and h(P,Q) for P* < P < P**

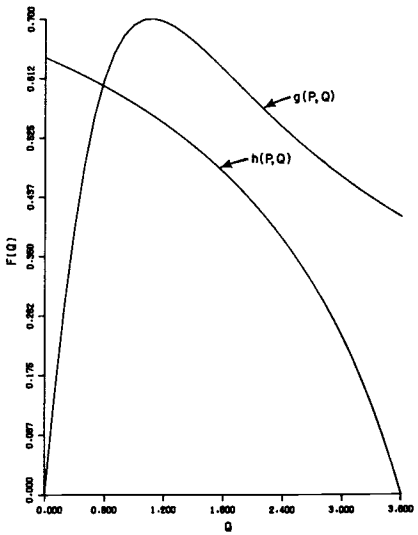

Figure 4c. Relation between g(P,Q) and h(P,Q) for P** < P

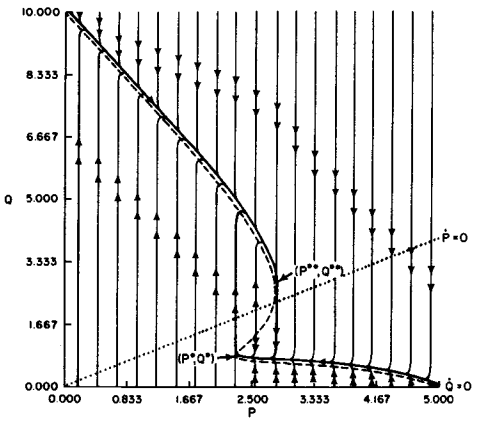

Figure 5. Flow in the (P,Q) state plane, showing fast flow perpendicular to slow manifold and relaxation oscillation

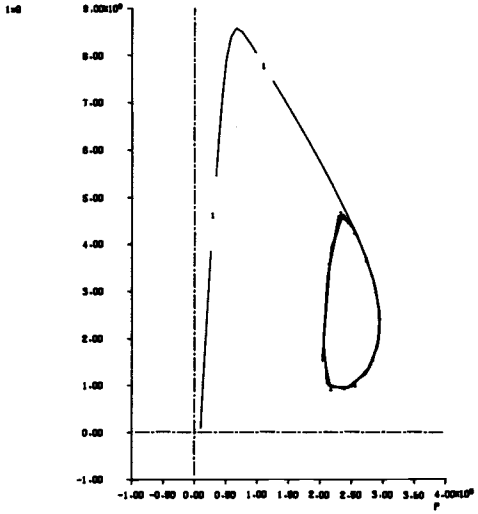

Figure 6a. State plane plot of P vs. Q for numerical integration of Eqs. 8 showing relaxation oscillation with all parameters the same as in Fig. 2 and $\varepsilon = \frac{1}{29.5}$. Gear's stiffly stable method was used for the integration and P(0) = 0.1, Q(0) = 0.1.

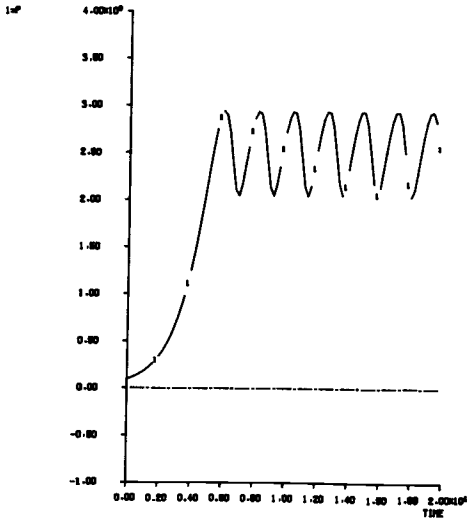

Figure 6b. Time trajectory plot of P for numerical integration of Eqs. 8

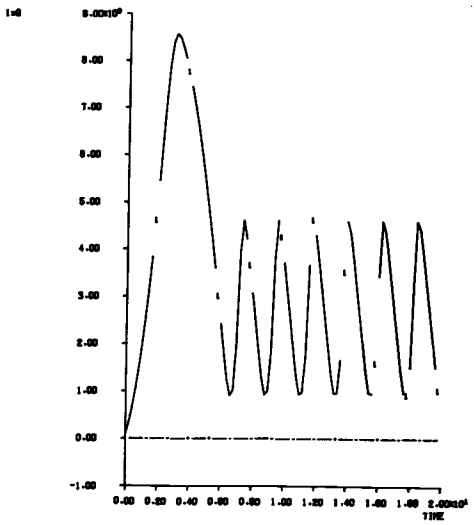

Figure 6c. Time trajectory plot of Q for numerical integration of Eqs. 8

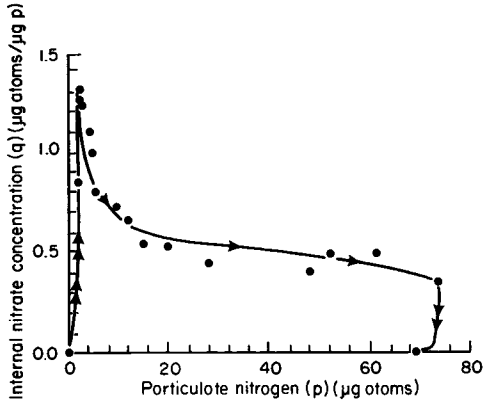

Figure 7. Replotting of data from DeMarche et al. (1979), Fig. 3, as a state space plot of particulate nitrogen, p, vs. internal nitrate pool, q, showing fast-slow transitions prior to extensive growth in p and prior to aborted oscillation. Fast transitions are shown as double arrows, while slow flow is shown as single arrows.

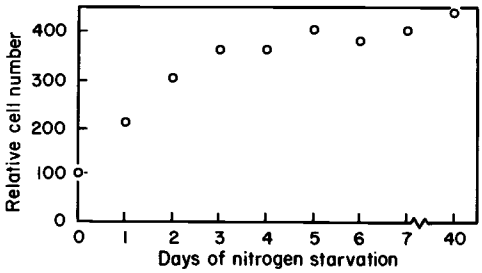

Figure 8. Replotting of data from Fogg (1975), Fig. 19, p. 56, showing oscillation of population size in a nitrogen limited batch culture during "steady state"